Epeleuton, a novel synthetic ω-3 fatty acid, reduces hypoxia/reperfusion stress in a mouse model of sickle cell disease

Alessandro Mattè,[1*] Enrica Federti,[1*] Antonio Recchiuti,[2*] Moayed Hamza,[3] Giulia Ferri,[2] Veronica Riccardi,[1] Jacopo Ceolan,[1] Alice Passarini,[1] Filippo Mazzi,[1] Angela Siciliano,[1] Deepak L. Bhatt,[4] David Coughlan,[3] John Climax,[3] Elisa Gremese,[5,6] Carlo Brugnara[7] and Lucia De Franceschi[1]

[1]Department of Medicine, University of Verona & AOUI Verona, Verona, Italy; [2]Department of Medical, Oral, and Biotechnology Science, "G. d'Annunzio" University Chieti Pescara, Chieti, Italy; [3]Afimmune Ltd., Dublin, Ireland; [4]Mount Sinai Heart, Icahn School of Medicine at Mount Sinai, New York, NY, USA; [5]Division of Clinical Immunology, Fondazione Policlinico Universitario A. Gemelli-IRCCS, Università Cattolica del Sacro Cuore, Rome, Italy; [6]Immunology Core Facility, Fondazione Policlinico Universitario A. Gemelli-IRCCS, Rome, Italy and [7]Department of Laboratory Medicine, Boston Children's Hospital, Department of Pathology, Harvard Medical School, Boston, MA, USA

AM, EF and AR contributed equally as first authors.

Correspondence: C. Brugnara
carlo.brugnara@childrens.harvard.edu

Received: August 11, 2023.
Accepted: December 7, 2023.
Early view: December 14, 2023.

https://doi.org/10.3324/haematol.2023.284028

SUPPLEMENTARY DATA

SUPPLEMENTARY METHODS

Organ collection and histological analysis, biochemical and hematological parameters. Organs were immediately removed and divided into two portions which were either immediately frozen in liquid nitrogen or fixed in 10% formalin and embedded in paraffin for histology. Paraffin-embedded tissue blocks were cut into 2-3 μm sections and mounted on adhesion microscope glass slides for Hematoxylin-Eosin (H&E), and Perls' staining for iron content. The analysis was performed on four different fields at a magnification of 200X. Tissue pathological analysis, inflammatory cell infiltrate, the presence of thrombi and iron deposition were carried out by blinded pathologists as previously described (1-3).
Hematological parameters were evaluated with a Sysmex XN-1000 Hematology Analyzer (Kobe, Japan) and red cell morphology was evaluated as previously reported (4-7). Biochemical assays were performed using standard biochemical assays, as previously reported (1, 8-11). Plasmatic Pentraxin 2 and CCL-2 and CXCL-2 were measured respectively using the Mouse Pentraxin 2/SAP Quantikine ELISA Kit (Biotechne, United states) and the next generation ELISA kit (ELLA multiplex cartridge; ProteinSimple, San Jose, CA, USA) according to the manufacturer's instruction.

Organ lipidomics. Analyses were carried out using an Agilent 1290 HPLC system coupled to an Agilent 6495 (for oxyplipins) or 6470 (for fatty acids) Triplequad mass spectrometer (Agilent Technologies, Santa Clara, USA) with electrospray ionization source was used and analyses were performed with Multiple Reaction Monitoring in negative mode, with at least two mass transitions for each compound.
Organs were excised end bloc and snap frozen in liquid N_2, stored at – 80 °C, and thawed at 4 °C prior to analysis. Samples (10-30 mg of tissue) were spiked with deuterium-labeled (d) internal standards (500 pg each, all purchased from Cayman Chemical, Ann Arbor, MI): 14,15-DHET-d11, 15-HETE-d8, 20-HETE-d6, 8,9-EET-d11, 9,10-DiHOME-d4, d4-12(13)-EpOME, d4-13-HODE, LTB4-d4. Methanol and NaOH were added for protein precipitation and alkaline hydrolysis (60 °C, 30 min). After centrifugation, the obtained supernatant was added to Bond Elute Certify II columns (Agilent Technologies, Santa Clara, USA) for solid phase extraction. The eluate was

evaporated on a heating block at 40 °C under a stream of nitrogen to obtain a solid residue. Residues were dissolved in 100 µL methanol/water. The residues were analyzed using an Agilent 1290 HPLC system with binary pump, multisampler and column thermostat with a Zorbax Eclipse plus C-18, 2.1 x 150 mm, 1.8 µm column using a gradient solvent system of aqueous acetic acid (0.05 %) and acetonitrile/methanol 50:50 (v/v). The flow rate was set at 0.3 mL/min, the injection volume was 20 µL. The HPLC was coupled with an Agilent 6495 Triplequad mass spectrometer (Agilent Technologies, Santa Clara, USA) with electrospray ionization source. Analysis was performed with Multiple Reaction Monitoring in negative mode, with at least two mass transitions for each compound. Internal standards were mixed to samples prior to extraction and consisted of: 14,15-DHET-d11, 15-HETE-d8, 20-HETE-d6, 8,9-EET-d11, 9,10-DiHOME-d4, d4-12(13)-EpOME, d4-13-HODE, LTB4-d4 (500 pg each) for analysis of oxylipins or C6:0-d11, C12:0-d23, C18:0-d35, C18:2-d4, C20:4-d11, C20:5-d5, C22:0-d43, C22:6-d5, C24:0-d4 (10 ng each) for analysis of fatty acid. All fatty acids were individually calibrated using Supelco 37-component FAME-Mix (Merck, Darmstadt, Germany) in relation to deuterated internal standards. For analysis of fatty acids, 100 µl of cell suspension were spiked with a mixture of deuterated internal standards (10 ng each), consisting of C6:0-d11, C12:0-d23, C18:0-d35, C18:2-d4, C20:4-d11, C20:5-d5, C22:0-d43, C22:6-d5, C24:0-d4 (Cayman Chemical, Ann Arbor, USA). NaOH (100 µL) and methanol (500 µL) were added and incubated for 120 minutes at 80 °C. Afterwards, 100 µl of acetic acid were added for neutralization. The mixture was filled with methanol and centrifuged. The clear solutions were analyzed using an Agilent 1290 HPLC system with binary pump, multisampler and column thermostat with a Kinetex C-18, 2.1 x 150 mm, 2.7 µm column using a gradient solvent system of aqueous acetic acid (0.05 %) and acetonitrile. The flow rate was set at 0.4 mL/min, the injection volume was 1 µL. The HPLC was coupled with an Agilent 6470 QQQ mass spectrometer (Agilent Technologies, Santa Clara, USA) with electrospray ionization source. Analysis was performed with Multiple Reaction Monitoring in negative mode, with at least two mass transitions for each compound. All fatty acids were individual calibrated using Supelco 37-component FAME-Mix (Merck, Darmstadt, Germany) in relation to deuterated internal standards. 3.3 Data Quality The dynamic range was determined prior to analysis. Based on these data, limits of quantification and coefficients of variation for the different lipid classes were determined and were in the lower pg/mL

range, depending on the analyte. The average coefficient of variation for a complete set of analytes was <15 %.

Immunoblot analysis. Packed red cells were lysed in ice-cold phosphate lysis buffer (5 mM Na_2HPO_4, pH 8.0, containing protease inhibitor cocktail tablets, 3 mM benzamidine final concentration, 1 mM Na_3VO_4 final concentration) and centrifuged 10 min at 4 °C at 12,000 *g*. Red cell membrane (ghost) and cytosol fractions were obtained as previously reported (6, 12). Frozen lung, kidney and aorta from each studied group were homogenized and lysed with iced lyses buffer (150 mM NaCl, 25 mM bicine, 0.1% SDS, 2% Triton X-100, 1 mM EDTA, protease inhibitor cocktail tablets (Roche), 1 mM Na3VO4 final concentration) then centrifuged 30 min at 4°C at 12,000 g (3, 13). Specific antibodies used are: anti Phospho-Tyrosine (clone PY99 from SCBT,Santa Cruz, CA (dilution 1:3000, 75 µg loaded) and clone 4G10 from Merck KGaA, Darmstadt, Germany (dilution 1:1600, 75 µgr loaded)); anti Phospho (Ser536) NF-kB p65 (dilution 1:1000, 75 µg loaded) and anti NF-kB p65 (clone C22B4) (dilution 1:1000, 75 µgr loaded) from Cell Signaling Technology (Danvers, MA, USA); anti-NLRP3/NALP3 from Vinci-Biochem Srl, Vinci, Italy (dilution 1:1000, 75 µgr loaded); anti Endothelin-1 (ET-1) form AbCam, Cambridge, UK (dilution 1:1000, 75 µgr loaded); anti VCAM-1 (R and D Systems, Minneapolis, MN, USA (dilution 1:1000, 40 µgr loaded)); anti ICAM-1 (clone EP1442Y, dilution 1:1000, 75 µgr loaded, AbCam, Cambridge, UK); anti TXAS-1 (Cayman, Ann Arbor, MI, USA); anti Nrf2-phospho-S40 (Clone EP1809Y, dilution 1:1000, 75 µgr loaded, AbCam, Cambridge, UK); anti-Nrf2 (dilution 1:1000, 75 µgr loaded, AbCam, Cambridge, UK); anti Nqo1 from Santa Cruz Biotechnology, Inc, CA, USA (clone C-19; dilution 1:1000, 75 µgr/ul loaded); anti-heme oxygenase 1(HO-1) form SCBT (Santa Cruz, CA, USA (dilution 1:1000, 50 µgr loaded); E-selectin (H-300) (dilution 1:1000, 75 µgr loaded); anti GAPDH from SCBT (Santa Cruz, CA, USA (dilution 1:5000, 50 µgr loaded)); anti Actin from SCBT (Santa Cruz, CA, USA (clone 2A3, dilution 1:1000, 50 µgr/loaded)). Secondary donkey anti-rabbit IgG (dilution 1:10000) and anti-mouse IgG (dilution 1:5000) HRP conjugated were from GE Healthcare Life Sciences (Little Chalfont, UK); secondary donkey anti goat IgG (dilution 1:10000) HRP conjugated was from SCBT, secondary donkey anti rat IgG (dilution 1:5000) HRP conjugated was from AbCam. Blots were developed with Luminata Forte Chemiluminescent HRP Substrate from Merk Millipore (Burlington, MA, USA), and images were acquired with the Alliance Q9 Advanced imaging system (Uvitec, UK). Densitometric analyses were performed with the Nine Alliance software (Uvitec, UK). Oxidized proteins were monitored by using the Oxyblot Protein Oxidation Detection Kit (EMD Millipore) following the manufacturer instructions (1).

Analysis of Efferocytosis and Macrophage Receptors. Following staining cells were fixed, permeabilized, and counter-labeled with Ter-119 FITC (Biolegend) to measure macrophage intracellular fluorescence associated with phagocytosed neutrophils and red cells respectively. Cells stained as above without permeabilization served as negative controls of intracellular staining, as previously reported (1). CD68 APC, and CD68 PE-Cy7 (Biolegend) were used to determine surface expression of phagocytic receptors on spleen and lungs macrophages identified using an anti-F4/80-APC-Cy7 antibody. Flow cytometry was carried out on a BD FACS Canto II (BD Biosciences, NJ, United States) and results were analyzed with the FACS DIVA software (BD Biosciences) (1).

Flow-cytometric analysis of total leukocytes and neutrophils .10 µl of heparinized blood was collected from anesthetized mice, RBCs were lysed with lysis solution (155 mM NH4Cl, 10 mM, KHCO3, 5% EDTA pH 7.4) for 10 min at RT, centrifuged at 300g for 5 min and washed twice with PBS BSA 1%. Freshly harvested spleens were mechanically disaggregated using the Gentle MACS dissociator (Miltenyi Biotec, Bergisch Gladbach, Germany) in 4 ml of PBS, BSA 1%, EDTA 2mM, filtered through a 70 µm cell strainer to obtain single cell suspension, stratified on the Lymphoprep™ Density gradient medium (Stem cell technologies, Vancouver, Canada), centrifuged at 800 g 20 min. The middle ring was collected and washed twice with PBS BSA 1% EDTA 2 mM. Cells from both blood and spleens were stained with CD16/CD32 blocking agent, CD45-eFluor450, Ly6G APC-eFluor780, B220 PE-Cy7, CD3 FITC, CD4 PE, CD8 PerCP-Cy5.5 (ThermoFisher Scientific, Waltham, United States) for 30 min at RT. After 1 wash with PBS BSA 1%, samples were resuspended in 200 µl of PBS BSA 1% added of the CountBright Absolute Counting Beads (ThermoFisher Scientific) and acquired with the Fortessa X-20 flow cytometer (BD Biosciences, Franklin Lakes, United States). The biparametric scatter plots were analyzed with FlowJo software version 10 (Tree Star Inc., Ashland, OR) (14).

References

1. Matte A, Recchiuti A, Federti E, et al. Resolution of sickle cell disease-associated inflammation and tissue damage with 17R-resolvin D1. Blood. 2019;133(3):252-265.
2. Rossato P, Federti E, Matte A, et al. Evidence of protective effects of recombinant ADAMTS13 in a humanized model of sickle cell disease. Haematologica. 2022;107(11):2650-2660.
3. Kalish BT, Matte A, Andolfo I, et al. Dietary omega-3 fatty acids protect against vasculopathy in a transgenic mouse model of sickle cell disease. Haematologica. 2015;100(7):870-880.

4. Kalish BT, Matte A, Andolfo I, et al. Dietary ω-3 fatty acids protect against vasculopathy in a transgenic mouse model of sickle cell disease. Haematologica. 2015;100(7):870-880.
5. Matte A, Federti E, Winter M, et al. Bitopertin, a selective oral GLYT1 inhibitor, improves anemia in a mouse model of β-thalassemia. JCI Insight. 2019;4(22).
6. Matte A, Low PS, Turrini F, et al. Peroxiredoxin-2 expression is increased in beta-thalassemic mouse red cells but is displaced from the membrane as a marker of oxidative stress. Free radical biology & medicine. 2010;49(3):457-466.
7. Brugnara C, Armsby CC, De Franceschi L, et al. Ca(2+)-activated K+ channels of human and rabbit erythrocytes display distinctive patterns of inhibition by venom peptide toxins. J Membr Biol. 1995;147(1):71-82.
8. Matte A, Federti E, Kung C, et al. The pyruvate kinase activator mitapivat reduces hemolysis and improves anemia in a beta-thalassemia mouse model. The Journal of clinical investigation. 2021;131(10).
9. Matte A, De Falco L, Iolascon A, et al. The Interplay Between Peroxiredoxin-2 and Nuclear Factor-Erythroid 2 Is Important in Limiting Oxidative Mediated Dysfunction in beta-Thalassemic Erythropoiesis. Antioxidants & redox signaling. 2015;23(16):1284-1297.
10. Brugnara C, de Franceschi L. Effect of cell age and phenylhydrazine on the cation transport properties of rabbit erythrocytes. J Cell Physiol. 1993;154(2):271-280.
11. de Franceschi L, Turrini F, Honczarenko M, et al. In vivo reduction of erythrocyte oxidant stress in a murine model of beta-thalassemia. Haematologica. 2004;89(11):1287-1298.
12. Matté A, Pantaleo A, Ferru E, et al. The novel role of peroxiredoxin-2 in red cell membrane protein homeostasis and senescence. Free Radic Biol Med. 2014;76:80–88.
13. Federti E, Matte A, Ghigo A, et al. Peroxiredoxin-2 Plays a Pivotal Role as Multimodal Cytoprotector in the Early Phase of Pulmonary Hypertension. Free Radic Biol Med. 2017.
14. Cossarizza A, Chang HD, Radbruch A, et al. Guidelines for the use of flow cytometry and cell sorting in immunological studies (second edition). Eur J Immunol. 2019;49(10):1457-1973.

Table 1S Lipidomics profile of livers from AA, SS, and SS mice treated with epeleuton

	AA Mice		**SS Mice**			**SS Mice + Epeleuton**		
pmol/100 mg of tissue	Mean	SD	Mean	SD	P value AA vs SS	Mean	SD	P value SS vs SS+Epe
Fatty Acids								
C8:0	3560.94	583.39	4641.75	908.48	ns	4698.81	1610.48	ns
C10:0	2156.66	384.88	2708.00	574.26	ns	3101.33	1617.82	ns
C12:0	6696.81	1881.91	7940.08	1916.07	ns	7394.23	1768.44	ns
C14:0	21469.12	12139.92	10713.43	3255.56	ns	7409.27	3018.76	ns
C15:0	8767.67	1306.82	7149.31	1709.94	ns	6270.80	1402.02	ns
C16:0	3734461.97	625912.12	2454065.39	170961.21	**0.029**	2372602.44	298362.62	**ns**
C16:1 n-7	334379.59	181440.54	131553.35	16722.82	**0.029**	123365.35	20514.58	**ns**
C17:0	16643.26	1694.46	13889.38	2261.13	ns	13258.87	2493.95	ns
C17:1 n-7	19840.08	7243.07	9914.92	395.52	ns	9805.75	706.35	ns
C18:0	1004375.39	69553.70	908802.75	131058.76	ns	876118.75	129822.83	ns
C18:1 n-9 cis	3483353.37	1469365.68	1612918.44	277776.58	**0.029**	1732132.65	239405.23	**ns**
C18:2 n-6 cis	3078584.61	476361.85	1500172.86	95782.43	**0.029**	1538180.21	244060.76	**ns**
C18:3 n-3	57434.17	22486.27	26735.37	3291.46	**0.029**	31487.02	6204.12	**ns**
C18:3 n-6	44625.10	9498.84	18450.06	1418.84	**0.029**	20498.28	4381.90	**ns**
C18:4	3485.14	1089.30	881.23	156.61	**0.029**	1291.10	636.17	**ns**
C20:0	27289.14	3613.13	5891.33	1249.13	**0.029**	3517.20	822.47	**0.029**
C20:1 n-9	73126.72	31847.71	30546.82	4455.85	**0.029**	23747.59	4528.55	**ns**
C20:2 n-6	32732.33	5865.15	29813.57	2610.45	ns	26569.99	1129.73	ns
C20:3 Σ	210100.13	47196.12	109635.86	14226.28	ns	113457.19	9435.28	ns
C20:4 n-3	8413.07	2730.79	3331.43	877.72	**0.029**	3862.44	680.84	**ns**
C20:4 n-6	1505466.19	83325.36	1368526.46	144183.36	ns	1236255.68	90621.82	ns
C20:5 n-3	27045.13	7897.86	21330.21	1200.87	ns	21874.25	3224.62	ns
C22:0	15499.70	3036.71	7294.38	1416.49	**0.029**	5083.44	1116.85	**ns**
C22:1 n-9	7702.47	2606.61	2835.79	462.24	**0.029**	2603.62	1269.28	**ns**
C22:2 n-6	2125.68	532.29	1045.98	193.15	**0.029**	794.25	71.32	**ns**

C22:5 n-3	101590.94	19187.95	72067.37	7703.10	**0.029**	65846.11	10574.58	**ns**
C22:5 n-6	76187.95	6616.08	83191.72	19942.76	ns	79529.13	17605.20	ns
C22:6 n-3	916550.35	107016.37	753417.69	61751.58	0.057	686833.52	65385.70	ns
C23:0	3083.26	882.92	4068.32	782.03	ns	3649.95	993.57	ns
C24:0	8332.81	2133.96	9425.34	2333.71	ns	7258.38	1595.07	ns
C24:1 n-9	10078.24	2147.61	20291.43	3353.78	**0.029**	15181.73	4440.74	**ns**
Oxylipins								
10-HDHA	14.99	5.46	12.58	2.38	ns	13.10	2.48	ns
11-HDHA	33.60	12.58	28.63	5.94	ns	28.36	5.35	ns
11-HEPE	0.57	0.10	0.52	0.09	ns	2.69	2.72	ns
12-HETE	191.48	41.62	263.31	94.10	**ns**	392.63	125.45	**0.047**
13-HDHA	23.08	8.67	18.11	4.40	ns	18.93	4.56	ns
14-HDHA	24.54	7.19	26.30	5.86	ns	30.91	6.23	ns
15-HEPE	1.57	0.40	2.04	0.87	**ns**	175.46	240.81	**0.029**
15-HETE	185.80	71.53	160.86	60.57	ns	163.40	44.59	ns
15-HeTrE	20.90	9.36	13.43	6.44	ns	28.99	10.56	ns
16-HDHA	28.88	14.14	21.99	7.95	ns	20.22	5.57	ns
16-HETE	6.33	2.26	6.29	1.61	ns	10.01	4.58	ns
17-HDHA	34.35	14.01	28.17	7.33	ns	29.35	8.50	ns
18-HEPE	3.79	1.06	3.30	1.41	ns	3.81	1.51	ns
19-HETE	5.03	6.18	4.34	1.23	ns	12.09	16.26	ns
20-HDHA	94.96	36.42	66.84	26.45	ns	73.85	23.39	ns
22-HDHA	2.09	0.63	2.00	0.35	ns	3.48	2.11	ns
4-HDHA	108.74	23.70	78.21	12.76	ns	106.77	19.62	**0.057**
5-HEPE	6.66	1.60	3.67	0.24	**0.029**	4.31	0.60	**ns**
5-HeTrE	1.94	0.79	2.28	0.49	ns	2.67	1.10	ns
7-HDHA	78.46	19.53	53.59	5.89	ns	74.19	12.84	ns
8-HDHA	52.02	15.24	38.78	3.29	ns	36.87	5.35	ns
8-HEPE	0.59	0.16	0.49	0.06	ns	0.69	0.30	ns
8-HETE	56.95	15.91	55.77	5.42	ns	49.92	1.48	ns
8-HeTrE	16.17	6.34	9.54	3.84	ns	10.18	3.02	ns

9-HETE	108.76	41.60	77.07	16.80	ns	99.68	22.95	ns
9-HODE	211.79	42.49	182.22	56.88	ns	288.87	113.38	ns
LTB4	0.42	0.16	0.40	0.10	ns	0.60	0.30	ns

Table 2S Lipidomics profile of spleens from AA, SS, and SS mice treated with epeleuton

	AA Mice		**SS Mice**			**SS Mice + Epeleuton**		
pmol/100 mg of tissue	Mean	SD	Mean	SD	P value AA vs SS	Mean	SD	P value SS vs SS + Epe
PUFA								
C8:0	7685.87	1671.26	6761.23	2734.17	ns	5921.25	3194.54	ns
C10:0	3644.03	1607.12	4333.45	1094.59	ns	4083.45	1904.18	ns
C12:0	10429.17	2683.43	11398.65	3752.49	ns	10270.35	2332.03	ns
C14:0	62181.90	4854.71	87430.58	14861.80	**0.034**	93098.88	24691.61	**ns**
C15:0	11647.90	1291.83	11963.28	1813.45	ns	11533.45	2674.60	ns
C15:1 n-5	0.00	0.00	0.00	0.00	ns	0.00	0.00	ns
C16:0	3374867.67	277685.38	3736278.18	299678.86	ns	3907380.53	460749.41	ns
C16:1 n-7	351688.87	29519.09	381204.48	30637.23	ns	438113.55	86948.50	ns
C17:0	10114.33	367.51	9810.88	1604.18	ns	9281.68	841.61	ns
C17:1 n-7	5710.07	558.58	6889.88	1247.21	ns	7451.65	2201.91	ns
C18:0	682697.90	67814.62	739501.93	98511.80	ns	698377.65	39692.00	ns
C18:1 n-9 cis	797071.33	173352.03	1137326.90	629980.68	ns	1135882.03	814300.09	ns
C18:2 n-6 cis	747521.13	57032.02	832013.98	298086.76	ns	846036.20	348293.47	ns
C18:3 n-3	14678.17	1989.07	18378.28	11227.41	ns	20019.40	15272.94	ns
C18:3 n-6	24771.37	2347.85	27303.70	5953.15	ns	23368.13	1914.79	ns
C18:4	1814.50	165.21	1865.95	488.78	ns	1484.05	391.14	ns
C20:0	9740.77	1400.73	7658.40	1429.77	ns	6324.58	1085.22	ns
C20:1 n-9	43801.47	3970.04	32189.98	7216.28	**0.077**	29595.90	8089.06	**ns**
C20:2 n-6	26921.40	1645.88	26202.65	3275.38	ns	25549.25	1686.07	ns
C20:3 Σ	98832.23	5427.74	75180.43	13480.79	**0.034**	63836.88	7965.78	**ns**
C20:4 n-3	1719.97	152.92	1344.53	263.91	**0.034**	1159.45	253.77	**ns**
C20:4 n-6	790875.53	59494.60	874982.13	86771.58	ns	893854.85	63371.62	ns

C20:5 n-3	9143.00	571.58	8202.90	1432.60	ns	7939.63	614.11	ns
C22:0	10453.47	530.48	7946.45	930.56	**0.034**	7232.40	800.18	**ns**
C22:1 n-9	9655.03	1362.52	7950.30	2707.91	ns	7015.88	673.54	ns
C22:2 n-6	5234.97	236.37	4232.60	336.07	**0.034**	4144.78	303.92	**ns**
C22:5 n-3	112624.17	14631.30	86125.18	3048.14	**0.034**	76391.98	3773.32	**0.021**
C22:5 n-6	66995.57	10579.01	69462.90	4109.83	ns	66903.53	16859.05	ns
C22:6 n-3	284514.57	37958.32	306021.15	32192.73	ns	312530.45	25218.99	ns
C23:0	3600.73	968.66	2248.53	565.82	ns	1881.60	167.14	ns
C24:0	13286.40	1252.94	12371.53	1389.30	ns	12143.88	2449.89	ns
C24:1 n-9	21022.23	530.76	18288.60	1241.03	ns	17949.63	1814.35	ns
Oxylipins								
10-HDHA	6.67	0.49	5.03	1.54	ns	8.60	7.10	ns
11-HDHA	6.77	0.65	6.93	1.28	ns	14.58	13.41	ns
11-HEPE	1.57	0.21	1.55	0.25	ns	2.78	1.78	ns
12-HETE	2866.53	273.93	1813.80	546.53	**0.034**	715.00	390.43	**0.043**
13-HDHA	12.33	0.84	17.28	2.79	**0.034**	19.50	6.67	**ns**
14-HDHA	71.40	19.48	57.20	59.83	ns	28.85	10.56	ns
15-HEPE	6.23	2.81	3.63	3.01	**ns**	132.13	147.18	**0.021**
15-HETE	225.57	7.70	313.20	80.22	**0.034**	238.05	75.93	**ns**
15-HeTrE	35.40	2.56	34.23	8.40	ns	47.65	16.04	ns
16-HDHA	9.93	0.96	11.03	0.85	ns	13.85	6.55	ns
16-HETE	2.87	0.55	2.73	0.50	ns	4.38	3.10	ns
17-HDHA	42.27	15.78	41.38	44.90	ns	26.15	7.71	ns
19-HETE	3.53	0.12	3.48	0.15	ns	3.48	0.53	ns
20-HDHA	26.63	4.10	30.65	5.16	ns	39.70	21.03	ns
22-HDHA	1.43	0.15	1.13	0.15	ns	1.85	0.75	ns
4-HDHA	21.70	4.16	23.48	5.61	ns	45.13	37.14	ns
5-HEPE	3.10	0.26	2.40	0.57	0.074	2.38	0.71	ns
5-HeTrE	1.53	0.21	1.28	0.33	ns	1.40	1.07	ns

7-HDHA	9.60	1.08	10.53	1.91	ns	20.75	19.75	ns
8-HDHA	7.27	1.22	8.73	2.12	ns	17.85	17.63	ns
8-HEPE	0.30	0.10	0.25	0.10	ns	0.33	0.19	ns
8-HETE	14.73	1.40	20.33	10.58	ns	32.20	22.87	ns
9-HETE	25.40	5.47	31.85	10.15	ns	39.08	20.10	ns
9-HODE	452.27	59.88	554.48	117.79	ns	502.03	235.13	ns
LTB4	5.27	1.76	3.50	1.32	**ns**	1.25	0.44	**0.021**

Table 3S. Effects of Epeleuton on lung, kidney, and liver pathology of sickle cell (SS) mice under normoxia and exposed to hypoxia/reoxygenation (H/R) stress			
	Normoxia	**H/R Vehicle**	**H/R Epeleuton**
Lung	(*n*=6)	(*n*=4)	(*n*=4)
Inflammatory cell infiltrates	8.8±0.7	96.8±8.2*	87.3±1.4*
Thrombi	0	0	0
Kidney	(*n*=6)	(*n*=4)	(*n*=4)
Inflammatory cell infiltrates	0	3.55±0.46*	4.2±0.01*
Thrombi	0	0	0
Liver	(*n*=6)	(*n*=4)	(*n*=4)
Inflammatory cell infiltrates	34.7±4.5	38.8±6.1	28.5±1.9
Thrombi	+ (4/6)	+(4/4)	0

H/R: hypoxia reoxygenation stress

Lungs

Score for inflammatory cell infiltrate. Quantification of inflammatory cell infiltrates was expressed as the mean of cells per field at magnification of X250, as resulting by the analysis of at least 10 different fields on each hematoxylin-eosin-stained whole lung section (see also refs: 28 and 29). Data are expressed as means±SEM; * p<0.05 compared to normoxia.

Thrombi: 0: no thrombi; +: presence of thrombi per field at magnification x250.

Kidney

Score for inflammatory cell infiltrate. Quantification of inflammatory cell infiltration in renal cortex of kidney was determined in hematoxylin-eosin-stained sections using a 0 to 4 scale based on the percentage of cell infiltrates occupied area in each field. 0 (no sign of infiltration); 1 (1-10% of the area with cell infiltration); 2 (11-25%); 3 (26-50%); 4 (50%). The mean of 15 randomly selected fields were analyzed at magnification X400 (see also refs: 22, 46). Data are expressed as means±SEM; * p<0.05 compared to normoxia; °p<0.05 compared to vehicle.

Thrombi: 0: no thrombi; +: presence of thrombi presence of thrombi per field at magnification x250.

Liver

Score for inflammatory cell infiltrate. Quantification of inflammatory cell infiltrates was expressed as the mean of cells per field at magnification of X250, as resulting by the analysis of at least 10 different fields on each hematoxylin-eosin-stained whole liver section (see also refs: 28 and 29). Data are expressed as means±SEM; * p<0.05 compared to normoxia.

Thrombi: 0: no thrombi; +: presence of thrombi presence of thrombi per field at magnification x250.

Statistical analysis: Non-parametric Pairwise Wilcoxon Rank Sum Tests were used.

SUPPLEMENTARY FIGURES

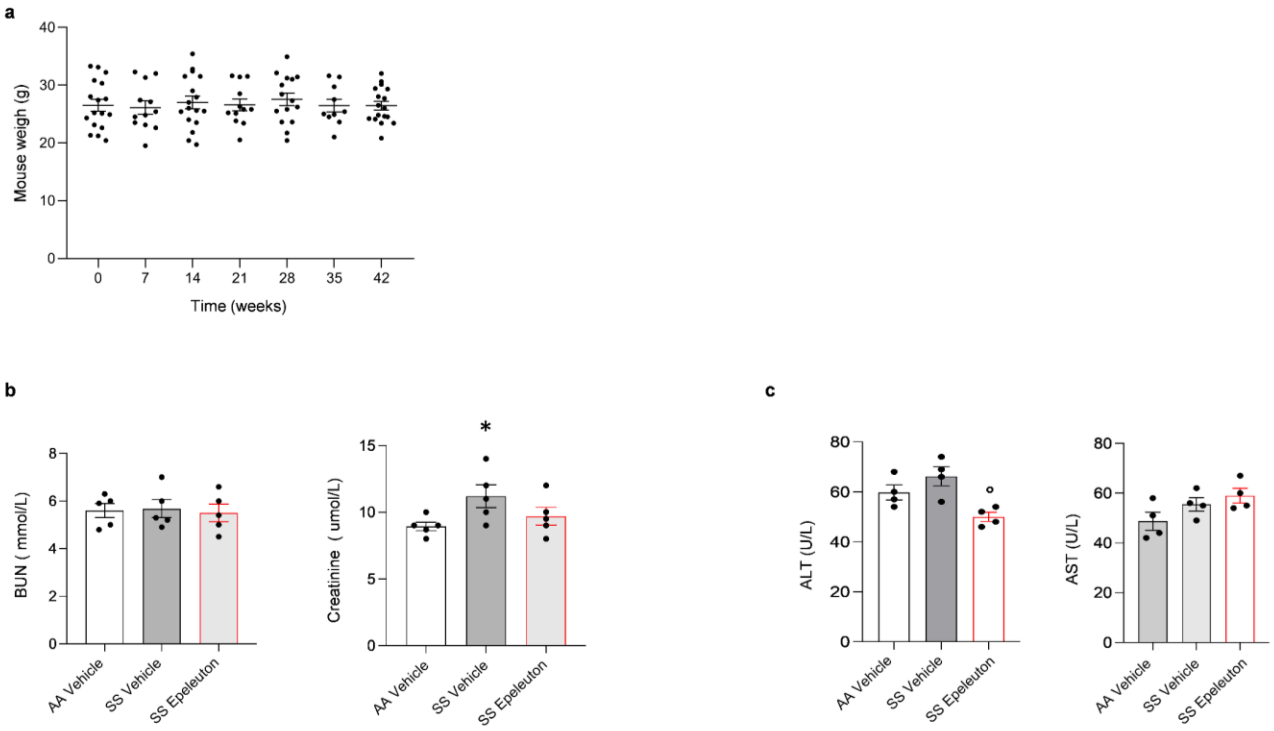

Figure 1S a. Weekly body weight measurement of SCD (SS) mice treated with epeleuton (1000 mg/Kg/d) for 6 weeks. Data are presented as mean ± SEM (n = 10-17). **b.** Plasma blood urea nitrogen (BUN) (left panel) and creatinine (right panel) in in healthy (AA) and SCD (SS) mice treated with either vehicle or epeleuton (1000 mg/Kg/d for 6 weeks). Data are presented as mean ± SEM (n = 5) by one-way ANOVA. * $p<0.05$ compared to AA mice. **c.** Plasmatic alanine transaminase (ALT, left panel) and aspartate transaminase (AST, right panel) in in healthy (AA) and SCD (SS) mice treated as in b. ° $p<0.05$ compared to vehicle by one-way ANOVA.

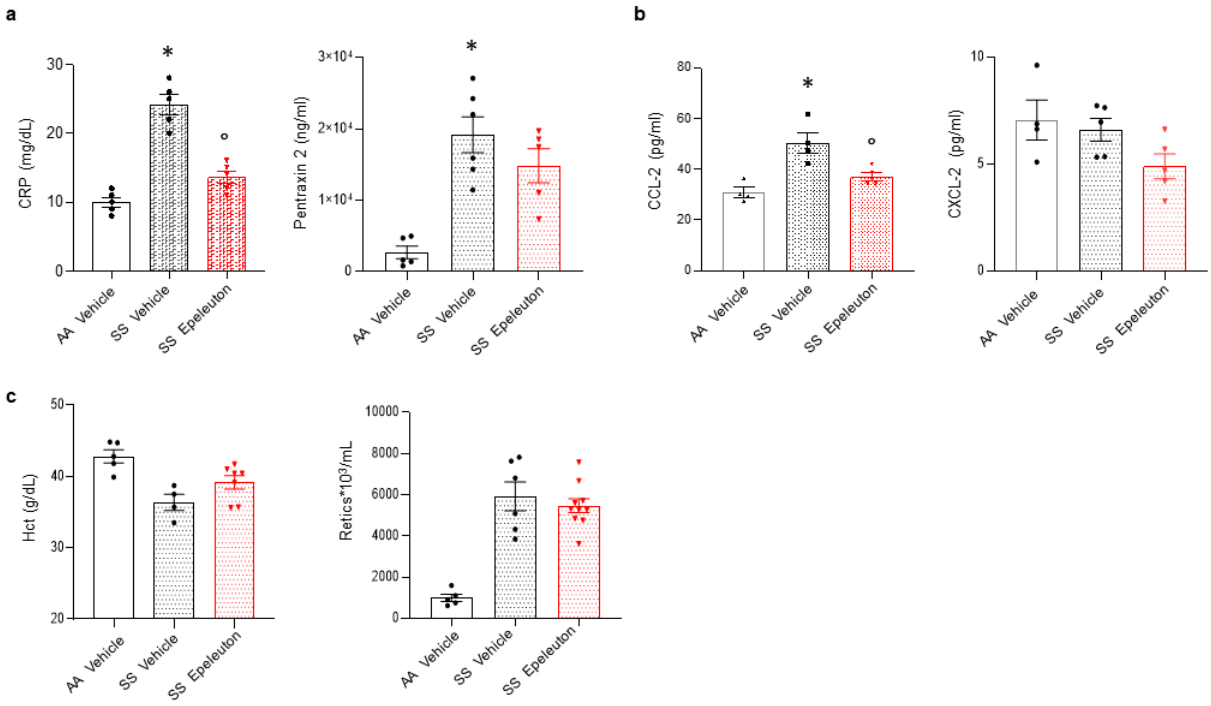

Figure 2S a. Plasmatic C-reactive protein (CRP, left panel), Pentraxin-2/SAP-1 (right panel) and **b.** plasmatic CCL-2 (left panel) and CXCL-2 (right panel) were evaluated in in healthy (AA) and SCD (SS) mice treated with either vehicle or epeleuton (1000 mg/Kg/day for 6 weeks). Data are presented as mean ± SEM (n = 4-6). * $p<0.05$ compared to AA mice. ° $p<0.05$ compared to vehicle by unpaired t-test with Bonferroni correction. **c.** Hematocrit level (Hct, left panel) and circulating reticulocytes count (retics, right panel) in in healthy (AA) and SCD (SS) mice treated with either vehicle or epeleuton (1000 mg/Kg/day for 6 weeks) under normoxia. Data are presented as mean ± SEM (n = 4-10) by unpaired t-test with Bonferroni correction.

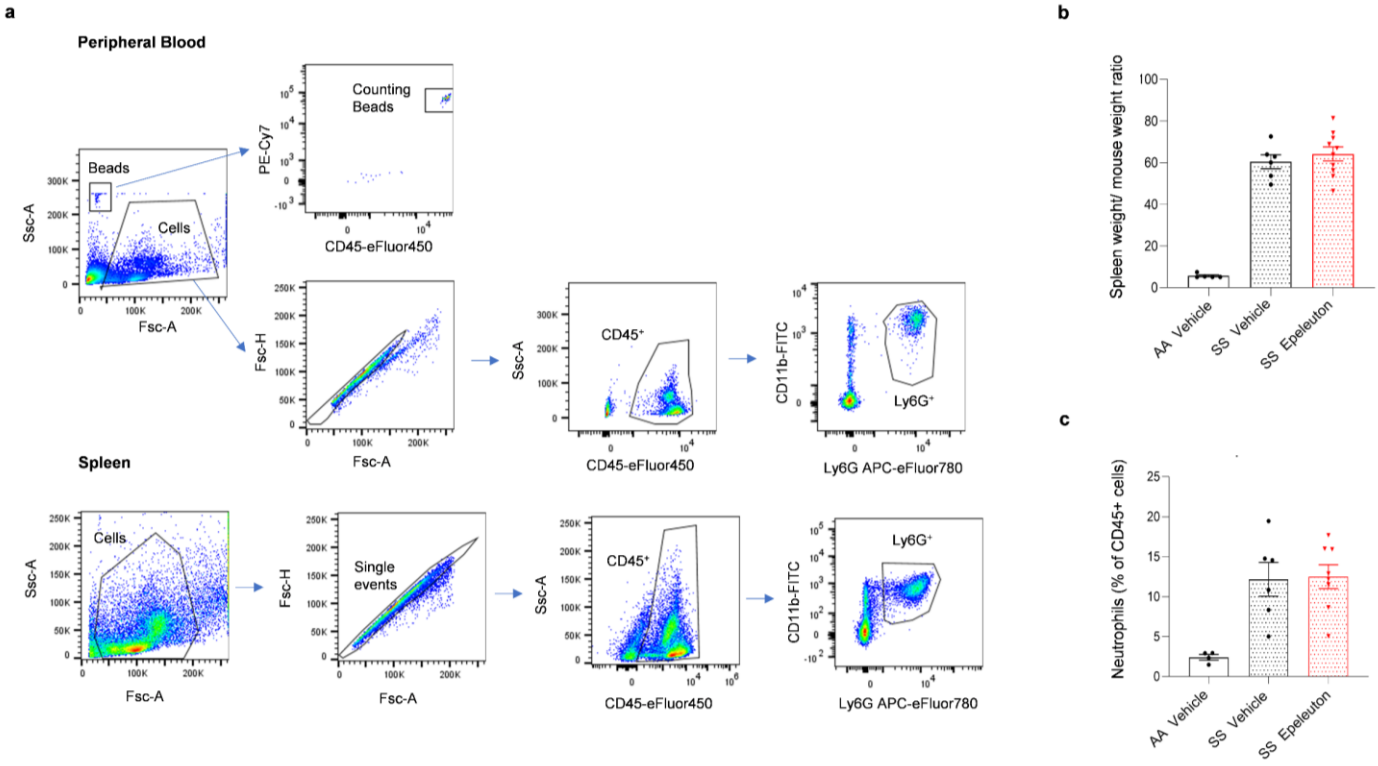

Figure 3S. a. Flow cytometric gating strategy for peripheral (upper panel) and spleen (lower panel) neutrophils identification. Neutrophils were recognized as CD45+Ly6G+ cells. **b-c.** Spleen weight/mouse weight ratio (b) and splenic neutrophils (c) identified by flow cytometric analysis as CD45+Ly6G+ cells in in healthy (AA) and SCD (SS) mice treated with either vehicle or epeleuton (1000 mg/Kg/day for 6 weeks). Data are mean ± SEM (*n* = 4-10).

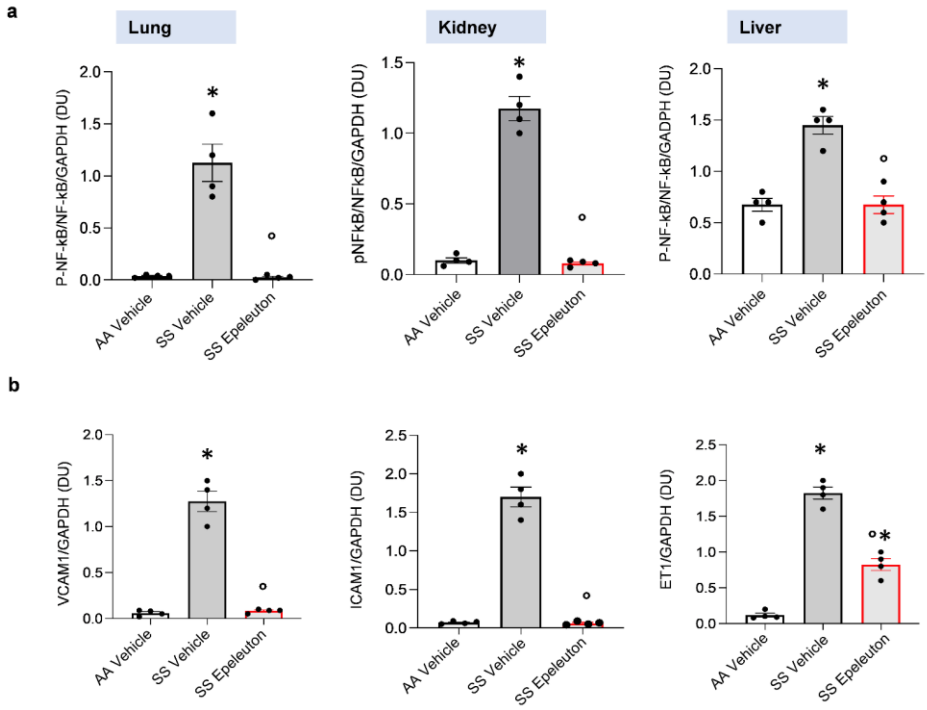

Figure 4S a. Densitometric analysis of immunoblots shown in Figure 2a-c. Data are presented as means ±SEM (*n*=4); * p<0.05 compared to AA mice; ° p<0.05 compared to vehicle (DU: Densitometric Unit). **b.** Densitometric analysis of immunoblots shown in Figure 2d. Data are presented as means ±SEM (*n*=4); * p<0.05 compared to AA mice; ° p<0.05 compared to vehicle by one-way ANOVA (DU: Densitometric Unit).

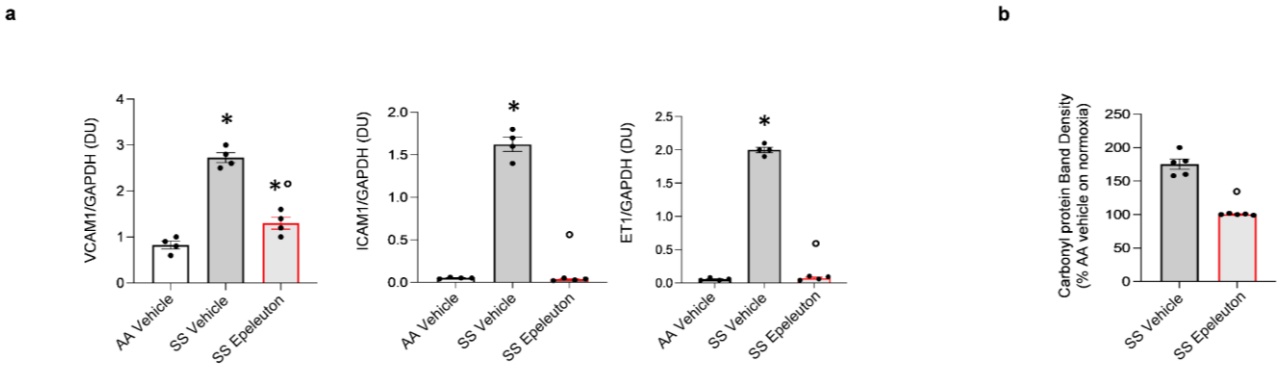

Figure 5S a. Densitometric analysis of immunoblots shown in Figure 2e. Data are presented as means ±SEM (*n*=4); * p<0.05 compared to AA mice; ° p<0.05 compared to vehicle by one-way ANOVA (DU: Densitometric Unit). **b.** Quantification of band area of Figure 2g. Data are presented as mean ±SEM (*n* = 5) (DU: Densitometric Unit). ° p<0.05 compared to vehicle.

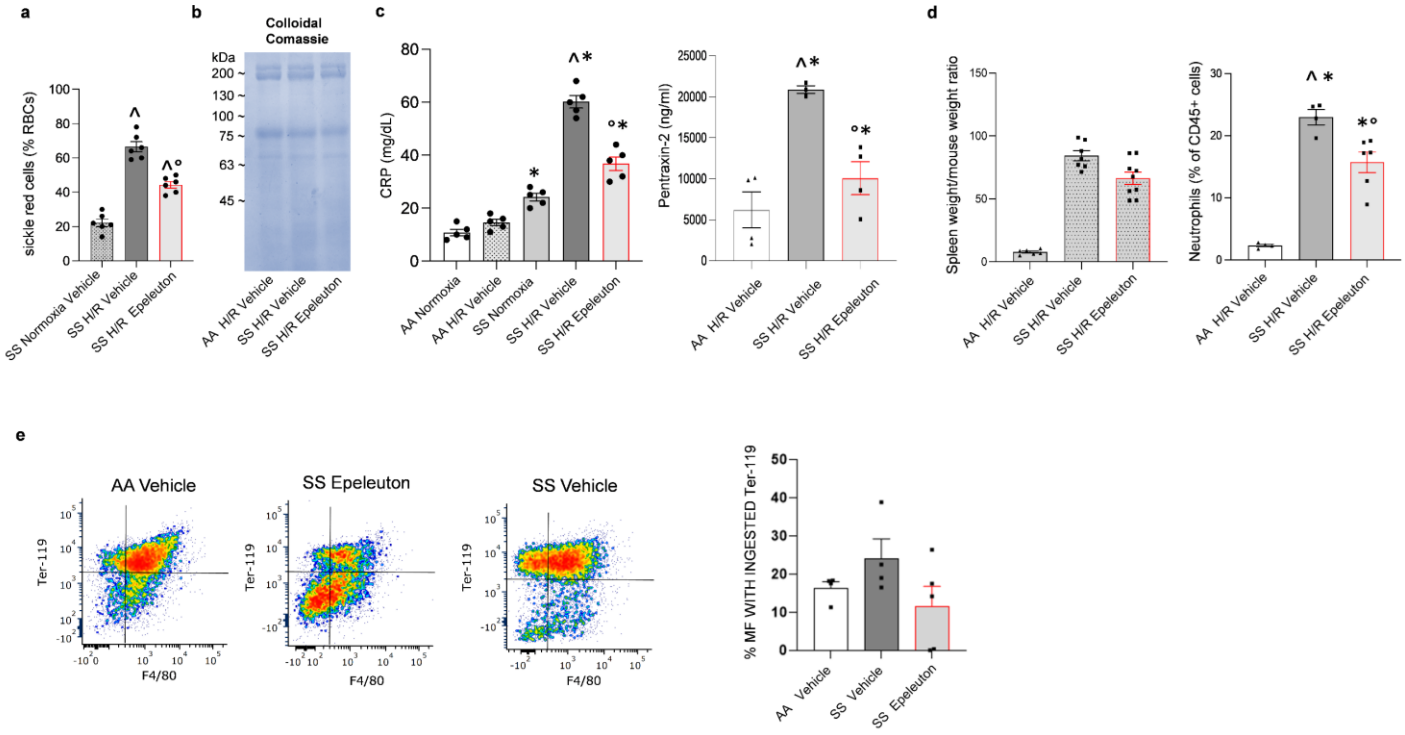

Figure 6S a. Quantification of the erythrocyte morphology from blood smear of SCD (SS) mice treated with or without epeleuton. Data are mean ± SEM (n=6). ^ p< 0.05 compared to normoxia, ° p<0.05 compared to vehicle treated mice by unpaired t-test with Bonferroni correction**. b.** Coomassie staining was used as loading control for Figure 3c. **c.** Plasmatic C-reactive protein (CRP, left panel), Pentraxin-2/SAP-1 (right panel) and **d.** spleen weight/mouse weight ratio (left panel) and splenic neutrophils (right panel) in in healthy (AA) and SCD (SS) mice exposed to H/R: hypoxia (8% oxygen; 10 hours), followed by reoxygenation (21% oxygen; 3 hours), treated with either vehicle or Epeleuton (1000 mg/Kg/d for 6 weeks). Data are presented as means ± SEM (*n*=4-9); * p<0.05 compared to AA mice; ° p<0.05 compared to vehicle. **e.** Phagocytosis of erythrocytes was assessed as the percentage of $F4/80^{+}$/$Ter\text{-}119^{+}$ double positive cells. MFI, Mean fluorescence intensities. Results are means ± SD (*n*= 4 mice/group); *p < 0.05 (one-way ANOVA).

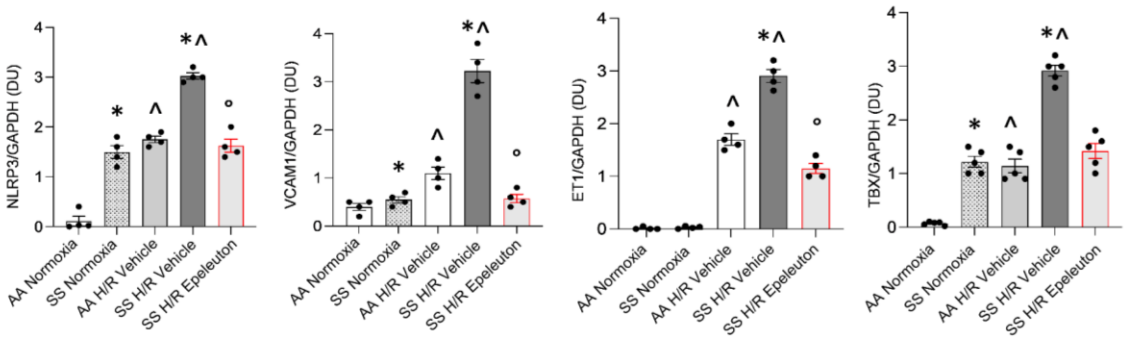

Figure 7S. Densitometric analysis of immunoblots Figure 5e. Data are presented as means ±SEM (*n*=4). * p<0.05 compared to AA mice; ^ p<0.05 compared to normoxia; ° p<0.05 compared to vehicle by one-way ANOVA (DU: Densitometric Unit).

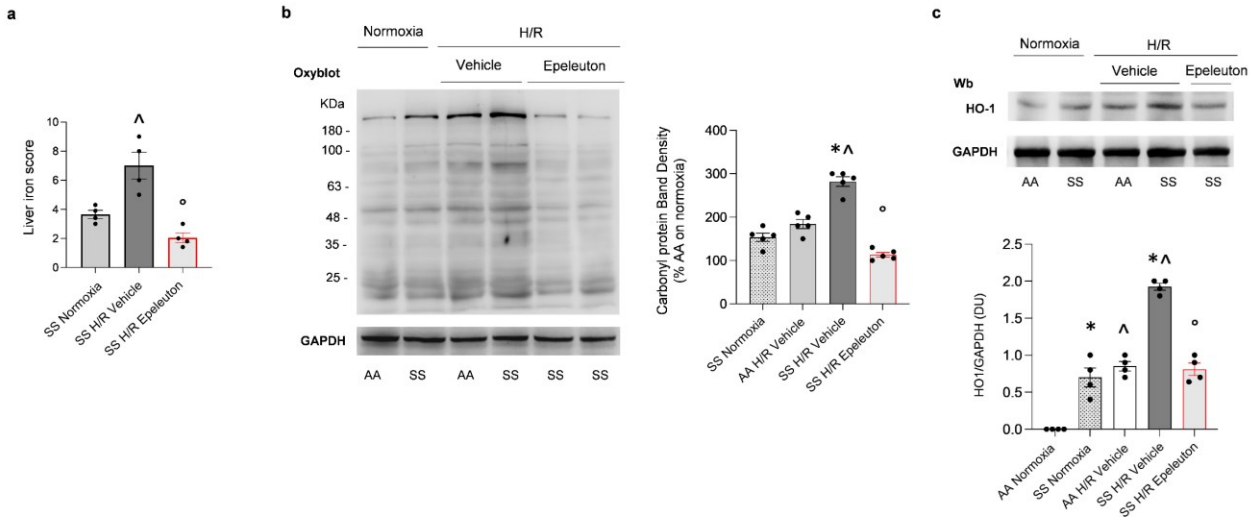

Figure 8S. a. Liver iron score in SCD (SS) mice treated with or without epeleuton. Data are mean ± SEM (n=4). ^ p< 0.05 compared to normoxia, ° p<0.05 compared to vehicle treated mice by unpaired t-test with Bonferroni correction**. b.** OxyBlot analysis of the soluble fractions of liver from in healthy (AA) and SCD (SS) mice under normoxia condition or exposed to H/R: hypoxia (8% oxygen; 10 hours), followed by reoxygenation (21% oxygen; 3 hours), treated with either vehicle or Epeleuton (1000 mg/Kg/d for 6 weeks). The carbonylated proteins (1 mg) were detected by treating with 2,4-dinitrophenylhydrazine and blotted with anti-DNP antibody. Quantification of band area is shown on the right. Data are presented as means ±SEM (*n*=5); * p<0.05 compared to AA mice; ^ p<0.05 compared to normoxia; ° p<0.05 compared to vehicle by one-way ANOVA. **c.** Immunoblot analysis using specific antibodies against HO-1 of liver from in healthy (AA) and SCD (SS) mice under normoxia condition or exposed to H/R: hypoxia (8% oxygen; 10 hours), followed by reoxygenation (21% oxygen; 3 hours), treated with either vehicle or Epeleuton (1000 mg/Kg/d for 6 weeks). 50 µg of protein loaded on an 11% T, 2.5%C polyacrylamide gel. GAPDH serves as protein loading control. One representative gel from 4 with similar results is shown. Densitometric analysis of immunoblots is shown on the right. Data are presented as means ±SEM (*n*=4); * p<0.05 compared to AA mice; ^ p<0.05 compared to normoxia; ° p<0.05 compared to vehicle by one-way ANOVA. (DU: Densitometric Unit).
GAPDH serves as protein loading control (**b** and **c**).

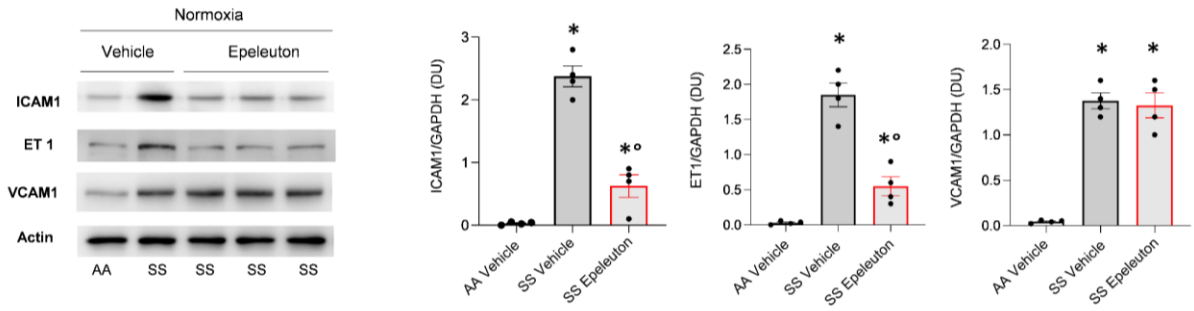

Figure 9S. Immunoblot analysis using specific antibodies against ICAM1, ET-1 and VCAM1 in isolated aorta from in healthy (AA) and SCD (SS) mice under normoxia treated with either vehicle or Epeleuton (1000 mg/Kg/d for 6 weeks). 75 µg of protein loaded on an 8% T, 2.5%C polyacrylamide gel. Actin serves as protein loading control. One representative gel from 4 with similar results is shown. Densitometric analysis of immunoblots is shown on the right. Data are presented as means ±SEM (*n*=4); * p<0.05 compared to AA mice; ° p<0.05 compared to vehicle by one-way ANOVA (DU: Densitometric Unit).